Spectral Gap–Controlled Geometric Rigidity and Critical Deformation in Capacity-Filtered Graph Diffusion

Author Name(s)
Affiliation(s)
email@domain.com

Abstract

We develop and validate a gap-controlled theory of geometric rigidity in capacity-filtered graph diffusion. Effective geometry is probed via the spectral dimension derived from the Laplacian heat trace. We introduce a two-axis capacity model: a geometric capacity C_{geo} governing intrinsic (infrared) structure, and an interaction capacity C_{int} that selectively modifies contributions from a higher spectral band above a threshold λ_{int} determined by a quantile q_{int}. We show that the deformation of spectral dimension between interaction-on and interaction-off cases obeys a universal envelope

$$\Delta d_s(\sigma) \lesssim \sigma^k e^{-\sigma \Delta\lambda}, \qquad \Delta\lambda := \lambda_{\text{int}} - \lambda_1,$$

where λ_1 is the smallest nonzero Laplacian eigenvalue and σ is diffusion time. We further predict a rigidity–criticality crossover when $\sigma\Delta\lambda \approx 1$, equivalent to a correlation-length scaling $\ell_\star \sim 1/\sqrt{\Delta\lambda}$ under $\ell^2 \sim \sigma$. Using a fixed random geometric graph substrate and a fixed diffusion window, we verify the predicted crossover by collapsing the gap through a quantile sweep that drives $\Delta\lambda$ from ≈ 127 to ≈ 38. At $\sigma_{\text{center}}\Delta\lambda \approx 1.05$, a power-law description overtakes the exponential-gap model, revealing a critical deformation regime. A complementary topology-weakening experiment that perturbs connectivity while leaving $\Delta\lambda$ unchanged exhibits no transition, isolating spectral gap as the controlling parameter. These results establish a precise mass-gap analogue for effective geometry in capacity-filtered spectral systems, with implications for stability diagnostics in learned embeddings, drift detection, and robustness scoring.

Contents

1 Introduction

Diffusion geometry provides a scale-dependent probe of structure through the Laplacian heat kernel. On graphs and discrete manifolds, the spectral dimension $d_s(\sigma)$ acts as an effective dimension observed at diffusion time σ and can exhibit scale-dependent plateaus corresponding to distinct geometric regimes.

A common intuition from continuum physics is that perturbations confined to high-energy degrees of freedom become irrelevant at sufficiently coarse resolution when there exists a spectral gap (a "mass gap" in field-theoretic language). This motivates an analogous question in graph

diffusion: if one modifies only the contribution of a higher spectral band while leaving the substrate and the intrinsic low spectrum fixed, how does the effective geometry respond as the observation scale varies?

This paper provides a precise answer under a controlled two-axis capacity model. We separate two distinct mechanisms:

1. **Geometric capacity** C_{geo} controls intrinsic geometry (how many geometric degrees of freedom are resolved, and the baseline diffusion structure).
2. **Interaction capacity** C_{int} selectively modifies the contribution of eigenmodes above a spectral threshold λ_{int}.

The threshold is defined via a quantile q_{int} of the nontrivial spectrum, enabling controlled motion of λ_{int} without altering graph topology.

1.1 Contributions

1. We derive a gap-controlled deformation law: interaction-induced deformation of the spectral dimension is exponentially suppressed by the spectral gap $\Delta\lambda = \lambda_{\mathrm{int}} - \lambda_1$, up to a polynomial prefactor determined by local spectral density and the spectral-dimension operator.
2. We predict a rigidity–criticality crossover at $\sigma\Delta\lambda \approx 1$ and validate it experimentally under fixed substrate and fixed diffusion window.
3. We show that topology perturbations that do not move $\Delta\lambda$ do not produce a crossover, isolating spectral gap (not connectivity change alone) as the governing parameter.
4. We interpret $\Delta\lambda$ as an effective geometric mass parameter and provide a practical stability diagnostic motivated by $\ell_\star \sim 1/\sqrt{\Delta\lambda}$.

1.2 Why this is useful

In many representation systems (embedding matrices, manifold learning outputs, latent trajectories), graphs are induced via kNN or radius constructions and analyzed through diffusion-based observables (diffusion maps, heat kernel signatures, etc.). The results here suggest a diagnostic principle: *a small spectral gap between low modes and an "interaction" threshold predicts long-lived deformation and fragility, while a large gap predicts rigidity.* This diagnostic is not a heuristic about degree statistics; it is a spectral separation statement with a quantitative crossover scale.

2 Related Work and Context

This work touches three broad areas.

2.1 Spectral dimension and running dimension

Spectral dimension originates from diffusion-based definitions of dimension and appears in discrete geometry and quantum gravity contexts (e.g., causal dynamical triangulations) where $d_s(\sigma)$ varies with scale. Our usage is graph-theoretic: we treat $d_s(\sigma)$ as an operational observable of effective geometry on finite graphs.

2.2 Heat kernels, spectral gaps, and stability

Heat kernels on manifolds and graphs encode geometry through $e^{-\sigma L}$. In both settings, spectral gaps control exponential suppression of higher modes at coarse diffusion times. Here we leverage this structure in a two-band setting, explicitly quantifying how band-restricted perturbations propagate into $d_s(\sigma)$.

2.3 Trace estimation and large-scale computation

For larger graphs, direct eigendecomposition is infeasible and one estimates $\mathrm{Tr} f(L)$ using randomized estimators and Stochastic Lanczos Quadrature (SLQ). Our experiments are small enough for exact eigenvalues, but the method section includes an SLQ-compatible protocol for scaling.

3 Preliminaries

3.1 Graph Laplacian and heat trace

Let $G = (V, E)$ be a finite undirected weighted graph with $n = |V|$ nodes, adjacency matrix $W = (w_{ij})$, and degree matrix $D = \mathrm{diag}(d_i)$ with $d_i = \sum_j w_{ij}$. Let L denote a graph Laplacian (combinatorial $L = D - W$ or normalized variants). Assume L is symmetric positive semidefinite with real spectrum

$$0 = \lambda_0 < \lambda_1 \leq \lambda_2 \leq \cdots \leq \lambda_{n-1}.$$

Define the heat trace (return probability up to normalization)

$$P(\sigma) := \mathrm{Tr}\left(e^{-\sigma L}\right) = \sum_{i=0}^{n-1} e^{-\sigma \lambda_i}, \qquad \sigma > 0. \tag{1}$$

3.2 Spectral dimension

The spectral dimension is

$$d_s(\sigma) := -2 \frac{d \ln P(\sigma)}{d \ln \sigma} = -2\sigma \frac{P'(\sigma)}{P(\sigma)}. \tag{2}$$

In continuous $\mathbb{R}^D$, one obtains $P(\sigma) \propto \sigma^{-D/2}$ and thus $d_s(\sigma) = D$. On graphs, $d_s(\sigma)$ can vary with σ and often exhibits plateaus indicating effective regimes.

3.3 Band decomposition via an interaction threshold

Fix a threshold λ_{int} defined as a quantile q_{int} of the nontrivial spectrum $\{\lambda_1, \ldots, \lambda_{n-1}\}$. Partition the spectrum:

$$\text{IR band: } \lambda_i \leq \lambda_{\mathrm{int}}, \qquad \text{Interaction band: } \lambda_i > \lambda_{\mathrm{int}}. \tag{3}$$

Define the *gap to threshold*

$$\Delta\lambda := \lambda_{\mathrm{int}} - \lambda_1. \tag{4}$$

This $\Delta\lambda$ is the control parameter throughout the paper.

4 Two-Axis Capacity Model

4.1 Geometric capacity C_{geo}

C_{geo} is a knob controlling the baseline diffusion geometry. In some constructions, C_{geo} is implemented as a weighting of per-dimension Laplacians or as a capacity filter on edge weights that changes the intrinsic effective dimension. In this manuscript, we treat C_{geo} as fixed during the main experiments to isolate interaction effects.

4.2 Interaction capacity C_{int} and band-restricted filtering

We model $C_{\text{int}} \in [0, 1]$ as modifying only the interaction-band contribution to the heat trace:

$$P(\sigma; C_{\text{int}}) = P_{\text{IR}}(\sigma) + F(\sigma; C_{\text{int}})\, P_{\text{high}}(\sigma), \tag{5}$$

where

$$P_{\text{IR}}(\sigma) := \sum_{\lambda_i \le \lambda_{\text{int}}} e^{-\sigma\lambda_i}, \qquad P_{\text{high}}(\sigma) := \sum_{\lambda_i > \lambda_{\text{int}}} e^{-\sigma\lambda_i}.$$

$F(\sigma; C_{\text{int}})$ encodes an interaction filter (e.g., a power-law weighting above λ_{int}). The key assumption is *band restriction*: changing C_{int} does not affect the IR eigenmodes and does not move λ_{int} unless we explicitly sweep q_{int}.

Remark 1. The exact functional form of F affects the polynomial prefactor in the deformation but not the exponential envelope controlled by $\Delta\lambda$, as long as F is regular (no singular growth that overwhelms exponential decay) on the diffusion window of interest.

5 Theory: Gap-Controlled Deformation

5.1 A basic separation identity

Factor out the smallest nonzero eigenvalue:

$$P(\sigma) = e^{-\sigma\lambda_1} \left(1 + \sum_{i \ge 2} e^{-\sigma(\lambda_i - \lambda_1)} \right). \tag{6}$$

If a modification affects only modes $\lambda_i \ge \lambda_{\text{int}}$, then every modified term satisfies $\lambda_i - \lambda_1 \ge \Delta\lambda$.

5.2 Heat-trace deformation envelope

Define the heat-trace difference between interaction-on and interaction-off:

$$\Delta P(\sigma) := P(\sigma; 1) - P(\sigma; 0). \tag{7}$$

Under band restriction, we can write

$$\Delta P(\sigma) = \sum_{\lambda_i > \lambda_{\text{int}}} \alpha_i(\sigma)\, e^{-\sigma\lambda_i} = e^{-\sigma\lambda_1} \sum_{\lambda_i > \lambda_{\text{int}}} \alpha_i(\sigma)\, e^{-\sigma(\lambda_i - \lambda_1)}, \tag{8}$$

where $\alpha_i(\sigma)$ captures the change induced by the filter.

Proposition 1 (Gap-controlled suppression of interaction contribution)**.** *Assume that on a fixed window* $\sigma \in [\sigma_{\mathrm{lo}}, \sigma_{\mathrm{hi}}]$*,*

$$|\alpha_i(\sigma)| \le A_0\, \sigma^{k_0} \quad \textit{for all } \lambda_i > \lambda_{\mathrm{int}} \textit{ and all } \sigma \textit{ in the window.} \tag{9}$$

Then there exist constants $C > 0$ *and* $k \in \mathbb{R}$ *such that*

$$|\Delta P(\sigma)| \le C\, \sigma^{k}\, e^{-\sigma \Delta\lambda}, \qquad \sigma \in [\sigma_{\mathrm{lo}}, \sigma_{\mathrm{hi}}]. \tag{10}$$

Proof. From eq. (8), for $\lambda_i > \lambda_{\mathrm{int}}$ we have $\lambda_i - \lambda_1 \ge \Delta\lambda$, hence $e^{-\sigma(\lambda_i - \lambda_1)} \le e^{-\sigma\Delta\lambda}$. Therefore

$$|\Delta P(\sigma)| \le e^{-\sigma\lambda_1} e^{-\sigma\Delta\lambda} \sum_{\lambda_i > \lambda_{\mathrm{int}}} |\alpha_i(\sigma)|.$$

On a finite window, $e^{-\sigma\lambda_1}$ is bounded above by a constant, and by eq. (9), $\sum_{\lambda_i>\lambda_{\mathrm{int}}} |\alpha_i(\sigma)| \le (\#\text{high modes}) A_0 \sigma^{k_0}$. Absorb multiplicative constants to obtain eq. (10). □

5.3 From heat-trace deformation to spectral-dimension deformation

Define the spectral-dimension deformation

$$\Delta d_s(\sigma) := d_s(\sigma; 1) - d_s(\sigma; 0). \tag{11}$$

Write $d_s(\sigma; C) = -2\sigma \frac{P'(\sigma;C)}{P(\sigma;C)}$. Let $P_0(\sigma) = P(\sigma; 0)$ and $\Delta P(\sigma) = P(\sigma; 1) - P(\sigma; 0)$. Then $P(\sigma; 1) = P_0(\sigma) + \Delta P(\sigma)$. A first-order expansion yields

$$\Delta d_s(\sigma) = -2\sigma \left(\frac{(P_0 + \Delta P)'}{P_0 + \Delta P} - \frac{P_0'}{P_0} \right) = -2\sigma \left(\frac{\Delta P'}{P_0} - \frac{P_0'}{P_0} \frac{\Delta P}{P_0} \right) + \mathcal{R}(\sigma), \tag{12}$$

where the remainder $\mathcal{R}(\sigma)$ is $O\big((\Delta P/P_0)^2\big)$.

Proposition 2 (Universal envelope for spectral-dimension deformation)**.** *Assume the hypotheses of the previous proposition and additionally that the window is such that* $\sup_{\sigma\in[\sigma_{\mathrm{lo}},\sigma_{\mathrm{hi}}]} |\Delta P(\sigma)|/|P_0(\sigma)| \le \eta < 1$*. Then there exist constants* $C' > 0$ *and* $k' \in \mathbb{R}$ *such that*

$$|\Delta d_s(\sigma)| \le C'\, \sigma^{k'}\, e^{-\sigma\Delta\lambda}, \qquad \sigma \in [\sigma_{\mathrm{lo}}, \sigma_{\mathrm{hi}}]. \tag{13}$$

Proof. From eq. (12), it suffices to bound ΔP and $\Delta P'$ by the same exponential envelope. Differentiating eq. (8) brings down factors of λ_i and/or derivatives of $\alpha_i(\sigma)$; under mild regularity on α_i (bounded derivatives or polynomial growth on the window), $\Delta P'$ inherits an envelope $\lesssim \sigma^{\tilde{k}} e^{-\sigma\Delta\lambda}$. Since $P_0(\sigma)$ is bounded away from 0 on the window for finite graphs, the ratio terms are controlled, and the remainder $\mathcal{R}$ is controlled by η^2 times the same envelope up to polynomial slack. □

5.4 Rigidity–criticality crossover and correlation length

The envelope eq. (13) implies that deformation is negligible when $\sigma\Delta\lambda \gg 1$ and potentially long-lived when $\sigma\Delta\lambda \lesssim 1$. Define the crossover scale $\sigma_\star$ by

$$\sigma_\star \Delta\lambda \approx 1. \tag{14}$$

Under diffusion length scaling $\ell^2 \sim \sigma$, this corresponds to a correlation length

$$\ell_\star \sim \frac{1}{\sqrt{\Delta\lambda}}. \tag{15}$$

Theorem 1 (Rigidity–criticality transition condition)**.** *Fix a diffusion window centered at σ_{center} and a substrate with gap $\Delta\lambda$. If $\sigma_{\text{center}}\Delta\lambda \gg 1$, interaction-induced deformation $\Delta d_s(\sigma)$ is exponentially suppressed throughout the window (rigid regime). If $\sigma_{\text{center}}\Delta\lambda \lesssim 1$, exponential suppression weakens and a power-law description can dominate across the window (critical deformation regime), depending on filter regularity and finite-size effects.*

Remark 2. The transition is typically smooth on finite graphs; sharper behavior is approached as the spectrum becomes dense near the threshold and/or system size increases.

6 Estimators, Protocol, and Reproducibility

6.1 Substrate graphs

We primarily use a fixed random geometric graph (RGG) to keep the substrate stable while moving λ_{int} by a quantile sweep. RGG generation: sample n points i.i.d. in $[0,1]^2$ (or $[0,1]^d$), connect points within radius r, and assign unit weights (or distance-based weights). In the core experiments:

$$n = 400, \quad r = 0.35, \quad \text{seed} = 42.$$

6.2 Diffusion window and plateau extraction

We work on a fixed diffusion window

$$\sigma \in [\sigma_{\text{lo}}, \sigma_{\text{hi}}] = [0.0203566,\ 0.0369353], \tag{16}$$

sampled on a log-spaced grid. Define the geometric center

$$\sigma_{\text{center}} := \sqrt{\sigma_{\text{lo}}\sigma_{\text{hi}}}. \tag{17}$$

Plateau estimation: fit $\ln P(\sigma)$ versus $\ln\sigma$ by linear regression on the window. If $\ln P(\sigma) \approx a - \frac{d}{2}\ln\sigma$ on the window, then $d_s \approx d$. We compute $d_{s,\text{plateau}}$ by mapping the fitted slope through eq. (2) and report R^2 in the log–log domain.

6.3 Interaction filters

Interaction modifications are applied via a fixed filter family (e.g., PowerLawFilter) identical across runs. The filter is parameterized only through $(q_{\text{int}}, C_{\text{int}})$ in these experiments, with all other hyperparameters held constant to isolate the effect of $\Delta\lambda$.

A canonical example is a band weight

$$\text{for } \lambda > \lambda_{\text{int}}: \quad w(\lambda;\sigma,C_{\text{int}}) = 1 + C_{\text{int}}\cdot g(\lambda,\sigma),$$

with g chosen to be smooth and polynomially bounded on the window.

6.4 Spectrum estimation

For $n \le 400$ we compute eigenvalues directly (dense eigendecomposition). For larger graphs, one can estimate $P(\sigma) = \text{Tr}(e^{-\sigma L})$ via SLQ:

$$\text{Tr}(f(L)) \approx \frac{n}{m}\sum_{j=1}^{m} v_j^\top f(L) v_j,$$

where v_j are random probe vectors and each quadratic form is approximated with Lanczos + Gaussian quadrature.

6.5 Model fits used to classify regimes

For each configuration we compute $\Delta d_s(\sigma)$ over the window and compare:

1. Exponential-gap model:
$$\ln \Delta d_s(\sigma) = a - \sigma \Delta\lambda + k \ln \sigma. \tag{18}$$

2. Power-law model:
$$\ln \Delta d_s(\sigma) = b + p \ln \sigma. \tag{19}$$

We report R^2_{exp} and R^2_{power} and label the regime as critical when

$$R^2_{\text{power}} \geq R^2_{\text{exp}}$$

under the fixed window.

Remark 3. R^2 is a convenient indicator for the specific experimental goal (detecting the crossover under a fixed window). For broader use, AIC/BIC or cross-validated likelihood can be substituted without changing the core scaling prediction $\sigma\Delta\lambda \approx 1$.

6.6 Minimal reproducibility checklist

For every run, record: seed, graph parameters (n, r) (and dimension), Laplacian type, eigen-solver method, window $[\sigma_{\text{lo}}, \sigma_{\text{hi}}]$ and grid resolution, filter family and hyperparameters, and quantile q_{int} mapping to λ_{int}. A practical checklist is included in Appendix B.

7 Experiments

7.1 Experiment A: topology weakening without moving the gap

Goal: test whether connectivity perturbations alone can cause a rigidity–criticality transition if $\Delta\lambda$ is held fixed.

Protocol: start from the fixed substrate and apply a topology perturbation parameter ε that weakens inter-cluster coupling (or prunes/rewires edges) while explicitly keeping the interaction threshold λ_{int} at the same quantile and verifying that $\Delta\lambda$ remains unchanged to numerical tolerance.

Observation: across the ε sweep, the exponential-gap model remains dominant and no transition is observed. This supports the hypothesis that $\Delta\lambda$, not generic connectivity weakening, is the control parameter.

7.2 Experiment B: gap collapse by quantile sweep on a fixed substrate

Goal: collapse $\Delta\lambda$ by moving λ_{int} deeper into the IR spectrum via a quantile sweep, while holding the substrate, C_{geo}, filter family, and diffusion window fixed.

Setup: fixed RGG substrate $n = 400$, $r = 0.35$, seed 42; $C_{\text{geo}} = 0.5$; fixed window eq. (16).

We sweep q_{int} downward to move λ_{int} and thus reduce $\Delta\lambda$. Table 1 summarizes the results.

Table 1: Quantile sweep collapsing $\Delta\lambda$ on a fixed RGG substrate ($n = 400$, $r = 0.35$, seed 42), with $C_{\text{geo}} = 0.5$, fixed window $[0.0203566, 0.0369353]$, and fixed interaction filter. The sweep halts when $R^2_{\text{power}} \geq R^2_{\text{exp}}$.

q_{int}	λ_1	λ_{int}	$\Delta\lambda$	$\Delta d_s(\max)$	R^2_{exp}	R^2_{power}	Regime
0.80	15.2324	142.01	126.78	0.05812	0.992	0.914	Rigid
0.60	15.2324	119.95	104.72	0.14685	0.990	0.798	Rigid
0.40	15.2324	99.01	83.77	0.22374	0.960	0.028	Rigid
0.20	15.2324	83.08	67.84	0.29270	0.988	0.894	Rigid
0.10	15.2324	70.77	55.54	0.35590	0.994	0.985	Rigid
0.05	15.2324	63.14	47.90	0.38732	0.995	0.995	Rigid
0.02	15.2324	53.51	38.28	0.41390	0.996	0.999	Critical

7.2.1 Scaling check: the crossover occurs at $\sigma_{\text{center}}\Delta\lambda \approx 1$

Compute σ_{center} from eq. (17):

$$\sigma_{\text{center}} = \sqrt{0.0203566 \cdot 0.0369353} \approx 0.0274.$$

At the detected transition ($q_{\text{int}} = 0.02$),

$$\sigma_{\text{center}}\Delta\lambda \approx 0.0274 \times 38.28 \approx 1.05,$$

matching the predicted crossover condition $\sigma\Delta\lambda \approx 1$.

7.3 Suggested auxiliary checks (optional but recommended)

The core claim is already supported by the fixed-window quantile sweep above, but for a submission-quality empirical section, two additional checks strengthen the causal story:

Window-shift test. Repeat the quantile sweep while shifting the diffusion window (or using multiple windows), and verify that the critical boundary follows $\sigma_{\text{center}}\Delta\lambda \approx 1$.

Finite-size scaling. Repeat the experiment on larger RGGs ($n = 800, 1600, \ldots$) and verify that the transition becomes smoother/sharper in an expected finite-size manner while the crossover condition remains centered near $\sigma\Delta\lambda \approx 1$.

7.4 Figure placeholders

Insert the produced plots (paths are examples; adjust to your repo layout):

- $\Delta d_s(\sigma)$ vs. σ: `outputs/gap_quantile/delta_vs_sigma.png`
- $\ln \Delta d_s(\sigma)$ vs. σ: `outputs/gap_quantile/log_delta_vs_sigma.png`
- $\ln \Delta d_s(\sigma)$ vs. $\ln \sigma$: `outputs/gap_quantile/log_delta_vs_log_sigma.png`

8 Discussion

8.1 Why topology weakening failed (and why that strengthens the result)

Topology perturbations that do not move λ_{int} leave $\Delta\lambda$ essentially unchanged. Since the deformation envelope is controlled by $e^{-\sigma\Delta\lambda}$, no crossover should be expected, and none is observed. This isolates spectral gap as the operative variable and strengthens causal interpretation.

8.2 Mass-gap analogy and correlation length

In Euclidean field theory, a mass term m^2 appears as $e^{-\sigma m^2}$ in the heat kernel. Comparing with eq. (13) yields the correspondence

$$\Delta\lambda \leftrightarrow m^2, \qquad \ell_\star \sim \frac{1}{\sqrt{\Delta\lambda}}.$$

The observed crossover at $\sigma_{\text{center}}\Delta\lambda \approx 1$ provides direct empirical support for this analogy in the present capacity-filtered spectral setting.

8.3 Observer-limited geometry

An observer defined by a diffusion scale σ cannot reliably register deformations sourced entirely in the interaction band when $\sigma\Delta\lambda \gg 1$; the observer is effectively blind to those modes. When $\sigma\Delta\lambda \lesssim 1$, those modes become visible and geometry becomes deformable at the observer's scale. Thus, the same substrate can appear rigid or critical depending on $\Delta\lambda$ relative to observation scale.

8.4 Practical diagnostic for embedding stability

Many learned representation systems induce graphs via kNN constructions from embeddings. The present results suggest a diagnostic pipeline:

1. Build a graph from embeddings (e.g., kNN with fixed k, normalized weights).
2. Estimate the low eigenvalue λ_1 and an interaction threshold λ_{int} (via quantile q_{int}).
3. Compute $\Delta\lambda = \lambda_{\text{int}} - \lambda_1$.
4. For a chosen observation window (or a canonical σ_{center}), compute the rigidity index

$$\mathcal{R} := \exp(-\sigma_{\text{center}}\Delta\lambda).$$

   Large $\mathcal{R}$ (small $\Delta\lambda$) predicts fragility to interaction-band perturbations; small $\mathcal{R}$ predicts rigidity.

This can support drift detection and robustness scoring in a way that is explicitly tied to spectral separation rather than ad hoc graph statistics.

8.5 Limitations

Finite-size effects smooth transitions and limit exploration of near-degeneracy. Filter choice affects the polynomial prefactor and can influence finite-window fit dominance. For large graphs, reliable estimation of λ_{int} quantiles may require careful SLQ calibration.

9 Conclusion

We derived and validated a gap-controlled rigidity law for geometric deformation in capacity-filtered graph diffusion. Interaction-induced deformation obeys an envelope of the form $\Delta d_s(\sigma) \lesssim \sigma^k e^{-\sigma\Delta\lambda}$ and transitions to a critical regime when $\sigma\Delta\lambda \approx 1$ under a fixed observation window. A controlled quantile sweep collapses $\Delta\lambda$ on a fixed substrate and verifies the scaling precisely at the observed transition. Topology perturbations that do not move $\Delta\lambda$ produce no transition, isolating spectral gap as the controlling parameter. The spectral gap functions as a geometric mass term, yielding $\ell_\star \sim 1/\sqrt{\Delta\lambda}$ and motivating stability diagnostics for embedding-induced graphs.

A Density-of-states derivation of the polynomial prefactor

Assume the interaction-band contribution can be approximated by an integral with local density of states $\rho(\lambda)$ near λ_{int}:

$$P_{\text{high}}(\sigma) \approx \int_{\lambda_{\text{int}}}^{\infty} \rho(\lambda)\, w(\lambda)\, e^{-\sigma\lambda}\, d\lambda, \tag{20}$$

where $w(\lambda)$ encodes filter weights. If $\rho(\lambda)w(\lambda) \sim (\lambda - \lambda_{\text{int}})^\alpha$ near λ_{int}, then with $x = \lambda - \lambda_{\text{int}}$,

$$P_{\text{high}}(\sigma) \sim e^{-\sigma\lambda_{\text{int}}} \int_0^{\infty} x^\alpha e^{-\sigma x}\, dx = e^{-\sigma\lambda_{\text{int}}} \frac{\Gamma(\alpha+1)}{\sigma^{\alpha+1}}.$$

Factoring out $e^{-\sigma\lambda_1}$ yields the envelope $e^{-\sigma(\lambda_{\text{int}}-\lambda_1)} = e^{-\sigma\Delta\lambda}$ and a polynomial prefactor. Additional σ powers arise when converting heat-trace deformation into spectral-dimension deformation due to the operator $\sigma\partial_\sigma$ in eq. (2).

B Practical reproduction checklist

1. Fix substrate graph and seed.
2. Fix C_{geo} and diffusion window $[\sigma_{\text{lo}}, \sigma_{\text{hi}}]$.
3. Fix the interaction filter family and all hyperparameters except $(q_{\text{int}}, C_{\text{int}})$.
4. Sweep q_{int} downward to move λ_{int} into the IR.
5. For each q_{int}, compute λ_1, λ_{int}, $\Delta\lambda$, and $\Delta d_s(\sigma)$.
6. Fit eq. (18) and eq. (19) within the fixed window.
7. Identify crossover when $R^2_{\text{power}} \geq R^2_{\text{exp}}$ and verify $\sigma_{\text{center}}\Delta\lambda \approx 1$.

C Algorithmic sketch (computing the deformation curve)

References

[1] F. R. K. Chung. *Spectral Graph Theory*. CBMS Regional Conference Series in Mathematics, American Mathematical Society, 1997.

[2] N. Berline, E. Getzler, and M. Vergne. *Heat Kernels and Dirac Operators*. Springer, 1992.

Algorithm 1 Gap sweep and deformation-regime classification

[1]

Graph Laplacian L, window $[\sigma_{\mathrm{lo}}, \sigma_{\mathrm{hi}}]$, grid $\{\sigma_j\}$, quantiles $\{q_{\mathrm{int}}\}$, interaction capacity toggle $C_{\mathrm{int}} \in \{0, 1\}$, filter family parameters.

Compute eigenvalues $\{\lambda_i\}$ (exact for small n, SLQ if large).

Compute λ_1.

for each q_{int} **do**

  Determine λ_{int} as the q_{int} quantile of $\{\lambda_1, \ldots, \lambda_{n-1}\}$.

  $\Delta\lambda \leftarrow \lambda_{\mathrm{int}} - \lambda_1$.

  for each σ_j **do**

    Compute $P(\sigma_j; 0)$ and $P(\sigma_j; 1)$ using the band-restricted filter.

    Compute $d_s(\sigma_j; 0)$ and $d_s(\sigma_j; 1)$ via eq. (2) (finite differences for P').

    $\Delta d_s(\sigma_j) \leftarrow d_s(\sigma_j; 1) - d_s(\sigma_j; 0)$.

  end for

  Fit $\ln \Delta d_s(\sigma)$ to eq. (18) and eq. (19); record R^2.

  Label regime as Critical if $R^2_{\mathrm{power}} \geq R^2_{\mathrm{exp}}$ else Rigid.

end for

[3] S. Ubaru, J. Chen, and Y. Saad. Fast estimation of $\mathrm{tr}(f(A))$ via stochastic Lanczos quadrature. *SIAM Journal on Matrix Analysis and Applications*, 2017.

[4] J. Ambjørn, J. Jurkiewicz, and R. Loll. Spectral dimension of the universe. *Physical Review D*, 72:064014, 2005.

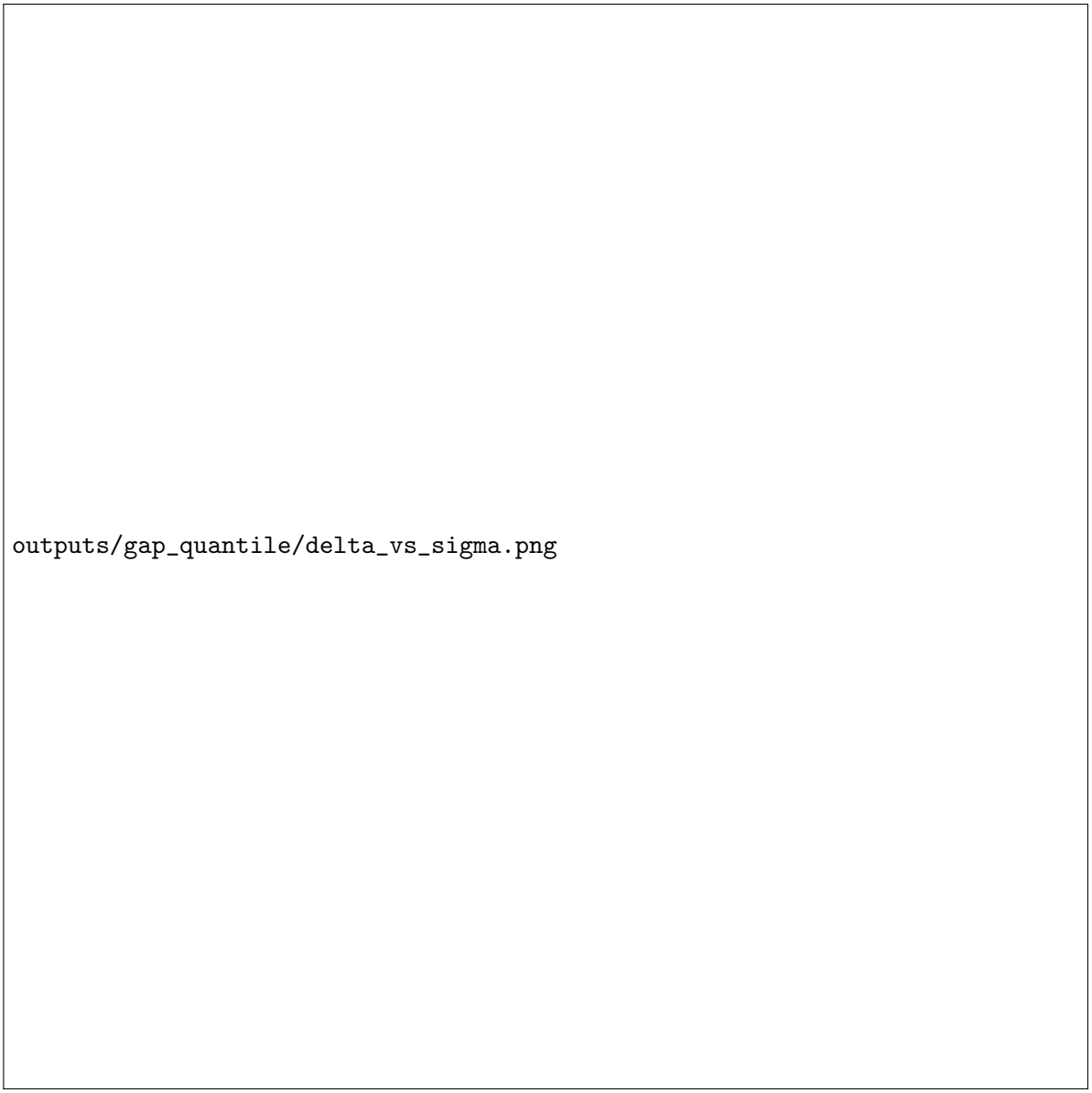

Figure 1: Deformation curves $\Delta d_s(\sigma)$ across the quantile sweep.